


Finite Element Investigation of the Bearing Capacity of Square Footings Resting on Sloping Ground

R. Acharyya¹ · A. Dey¹ 

Received: 28 April 2017 / Accepted: 28 July 2017 / Published online: 8 August 2017
© Indian National Academy of Engineering 2017

Abstract The ultimate bearing capacity of foundation placed on a slope is significantly affected by its vicinity to the slope face, which offers substantially lesser passive resistance as compared to a footing resting on a semi-infinite medium. Conventional bearing capacity theories fail to address the behavior of such foundations. Few existing theories predict the bearing capacity of foundations on slopes considering stress-based failure approach. However, deformation along the slope plays a major role in governing the failure of such foundations, thus requiring a coupled stress-deformation based failure analysis. With the aid of 3-D finite element modelling, employing coupled stress-deformation analysis, this study addresses the failure mechanism and the bearing capacity (q_u) of a square footing located on a dry cohesionless slope. The effect of various parameters, namely the angle of internal friction of soil, setback distance, slope inclination, footing width and the depth of embedment of the footing, have been investigated. Variations parameters are found to noticeably alter the bearing capacity estimate and the observed failure mechanism. A critical setback distance is obtained [$(b/B)_{\text{critical}} = 3$] beyond which the failure mechanism resembles the same obtained for a footing resting on horizontal ground. The unit weight and modulus of elasticity of the soil material is found to have negligible effect on the bearing capacity.

Keywords Square footing · Bearing capacity · Setback distance · Slope inclination · 3-D finite element

List of Symbols

b	Setback distance
c	cohesion
E_s	Elastic modulus of soil
q	Applied pressure over footing
q_u	Bearing capacity
b/B	Setback ratio
B	Width of footing
D	Embedment depth of footing
D/B	Embedment ratio
$N_\gamma, N_{\gamma q}$	Bearing capacity factors
ϕ	Angle of internal friction
ψ	Dilatancy angle
ν	Poisson ratio
γ	Unit-weight of soil
γ_{dmax}	Maximum dry-density of soil
β	Slope angle

Introduction

The bearing capacity of the foundations is a primary concern for geotechnical engineers as it helps in the evaluation and design of a safe foundation. Design of foundations on a horizontal ground surface depends on the mechanical characteristics of the soil (unit weight and shear strength parameters) and the physical properties of the foundation (depth, width, and shape of the footing). There are two primary considerations to decide the allowable bearing pressures of shallow foundations (a) the safety factor against ultimate shear failure must be adequate, and (b) the settlements should not exceed the tolerable limits.

✉ A. Dey
arindamdeyitg16@gmail.com

R. Acharyya
r.acharyya@iitg.ernet.in

¹ Department of Civil Engineering, Indian Institute of Technology Guwahati, Guwahati, Assam, India

Conventionally, the ultimate bearing capacity of foundation is defined as the maximum stress that it can carry without undergoing a shear failure. Based on the shear strength parameters of the soil, Terzaghi (1943) was the first to quantify the ultimate bearing capacity of a strip footing resting on a uniform horizontal ground, which is used extensively even today. The basic proposition for the bearing capacity of strip footings has undergone several modifications, primarily related to the theoretical bearing capacity factors, as well as inclusion of several new contributory factors (Meyerhof 1957; Vesic 1973; Hansen 1970). However, strip footings are not commonly used as building foundations, except for the load bearing walls. Hence, in order to accommodate different shapes of the footings (square, rectangular, circular or combined), shape factors were introduced in the bearing capacity expressions (Vesic 1973; Hansen 1970).

Rapid growth of urbanization in the North-Eastern hilly regions of the country has resulted in myriads of residential and commercial constructions. The foundations of such constructions are mostly shallow, and are located either on the crest or on the benched face of the slopes. Apart from the urban constructions, transmission towers, water tanks, retaining walls, footings for bridge abutments, and even foundations for transportation links are mostly located on the slopes. Foundation on slopes is a challenging and complex problem for the geotechnical engineers. The stability of a footing located on or near a slope is affected by its location, the loading pattern, the edge distance from the slope face, the slope angle, the depth of embedment of the footing, the shear strength characteristics of the foundation soil and other factors, such as the rainfall, seismicity and saturation level of the foundation material. For footing placed near to face of a slope, a reduction in the bearing capacity of the foundation is expected due to the curtailed zone of passive resistance developed towards the slope face.

There are several literature addressing the theoretical analysis of bearing capacity of strip footing resting on horizontal ground (Choudhury and Rao 2005; Pain et al. 2016; Ghosh and Choudhury 2011), as well as on slopes (Kumar and Rao 2003; Kumar and Ghosh 2006; Choudhury and Rao 2006; Kumar and Chakraborty 2013; Chakraborty and Kumar 2014). It is observed that in contrast to the footings resting on horizontal ground (Zhu and Michalowski 2005, Cerato and Lutenegeger 2006, 2007; Yu et al. 2010; Lavasan and Ghazavi 2014), there exists limited reports on experimental investigations related to the estimation of the bearing capacity of a footing located on a slope (Shields et al. 1977; Bauer et al. 1981; Kumar and Ilampurthy 2009; Castelli and Lentini 2012; Azzam and Farouk 2010; Keskin and Laman 2013). Most of the attempts have been made to evaluate the bearing capacity

of a strip footing, resting on dry cohesionless sandy soil slope, and to investigate the effects of the governing parameters (Setback distance defined as the distance of the footing from the edge of the slope crest, width of the footing, relative density of slope material, steepness of the slope and type of loading on the footing). Very few literature exist related to the laboratory investigations for square and circular footings resting on a slope (Castelli and Lentini 2012; Azzam and El-Wakil 2015; Shukla and Jakka 2016).

Habitats in the hilly regions mostly comprise of the houses resting either on the slope face or on the slope crest. A 'Compilation of the catalogue of the building typologies in India' revealed that most of the buildings located in the hilly terrains in the North-Eastern regions of India are supported by shallow isolated footings (NDMA 2013). Hence, it is important to address and understand the mechanism of failures of shallow isolated square footings resting on the hill-slope. However, very limited literature exists in this regard. Castelli and Lentini (2012) reported an experimental study for a square footing placed on the crest of a dry sandy slope, solely to study the effect of footing width and setback distance on its ultimate bearing capacity and the associated bearing capacity factor. As mentioned earlier, several other parameters govern the response of foundation on slopes, the cumulative effect of which remains unaddressed. Hence, based on 3-D finite element (FE) simulations using PLAXIS 3D AE.01, this article reports the effect of various geotechnical and geometrical parameters on the ultimate bearing capacity of a square footing resting on or near the slopes. The 3D numerical model also provides a description of the failure mechanism involved in the process of loading and failure of the footing.

Description of the Problem

Finite element 3-D analysis has been carried out to study the behavior of a shallow square footing resting on a dry cohesionless soil slope, with an aim to represent the commonly occurring building foundations in the hill slopes of North-Eastern India. Hill-slopes of this region comprises of different types of soils, ranging from fine silts, marginal soil mixtures, gravels, as well as highly weathered rock masses. Hence, although purely cohesionless slopes are not found in this region, the present study provides a good insight into the failure mechanism of the slopes made up of the cohesionless materials as the dominant component (weathered rocks either as semi-massive boulders or in the size fractions of gravel and sand), when subjected to human intervention and construction activities. Moreover, laboratory investigations of such problems, as model or prototype

experimentations, mostly uses cohesionless sandy material for the ease of construction and control (Shields et al. 1977; El-Sawwaf 2005, 2010; Keskin and Laman 2013; Castelli and Lentini 2012; Turker et al. 2014). The difficulty in conducting large number of laboratory experimentations by considering the variations of different parameters can be overcome through a validated numerical model encompassing parametric variations. Thus, although the study does not incorporate the varying natural composition of locally available soil, the insights about the failure mechanism obtained from the study is useful for special conditions and experimental simplifications. Although it is understood that the stability of such cohesionless soil slopes will be largely affected by climatic conditions, the incorporation of the same is beyond the content of this article. The following sections provide the details of the various aspects of the numerical modeling adopted for the present study.

Geometry and Boundary Conditions

The model geometry has been developed for footing located on the crest or the face of the slope, as shown typically in Fig. 1. In accordance to the Boussinesq’s elastic stress theory, the “ $0.1q$ ” (q is the stress applied on the footing up to its failure) stress contour represents the outermost significant isobar, beyond which the effect of the applied stress is considered negligible. The model dimensions have been so chosen that the significant isobar is not intersected by the model boundaries (Fig. 2). In the numerical model, “standard fixity” condition has been employed. Horizontal fixity was applied to the lateral vertical edges, while the bottom edge of the model is assumed to be non-yielding and restrained from both vertical and horizontal movements (Fig. 3). The inclined slope face is devoid of any fixity, allowing for free deformation occurring due to the location and loading of the footing.

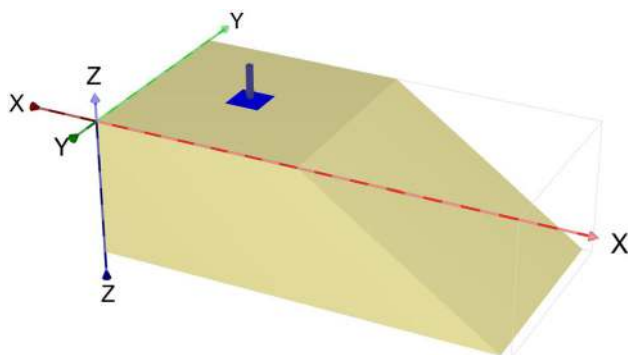


Fig. 1 Typical PLAXIS 3D representation of a footing resting on the crest of a slope

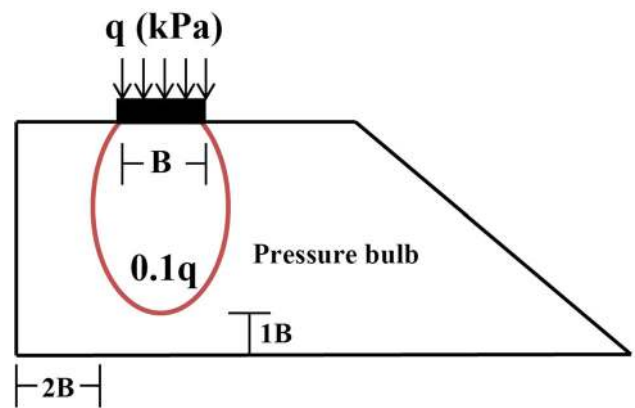


Fig. 2 Schematic representation of a model geometry for a footing resting on sloping ground (not to scale)

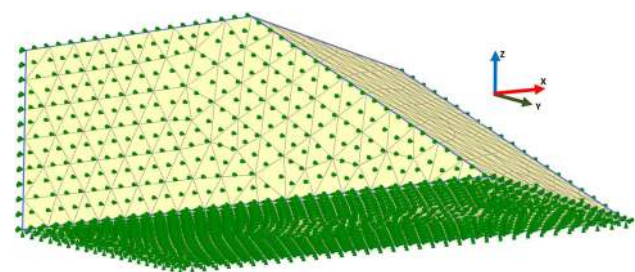


Fig. 3 Standard fixities applied in the numerical model

Finite Element Meshing

To perform the finite element computation, the model was discretized into smaller finite number of 10-noded tetrahedral elements. The meshing of the domain is carried out based on the fully automatic generation of finite elements inherent to the PLAXIS 3D program. Five basic meshing schemes are available (namely, very coarse, coarse, medium, fine, and very fine mesh), while allowing the user for further refinements of a region, around a line or around a node. The typical meshing obtained for a numerical model is shown in Fig. 4. A very coarse mesh fails to capture the

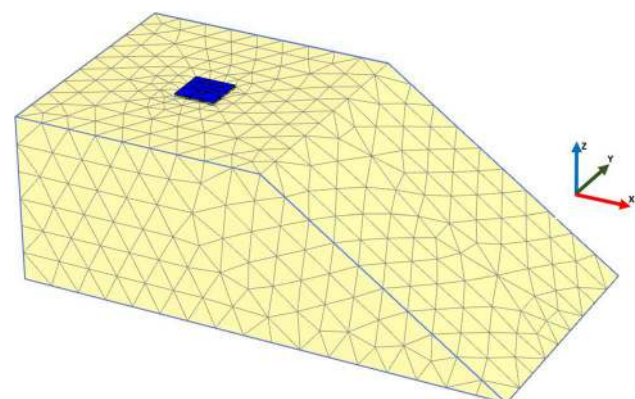


Fig. 4 Typical meshing scheme adopted in the numerical model

important characteristic responses of the domain. Beyond optimally fine meshes, there are chances of the accumulation of numerical errors, thereby producing inaccuracy in the obtained information. Moreover, very fine meshing is also affected by excessive computation time. Hence, a convergence study should be conducted to determine the optimum mesh configuration for any simulation model.

Location of the Footing

In order to estimate the bearing capacity of footing in the numerical framework, various locations of a square footing have been chosen for the numerical analyses. Figure 5 shows the different locations of the surface and embedded footings on the crest or the face of the sloping ground.

Material Model

The cohesionless soil is modelled by the linear elastic perfectly-plastic Mohr–Coulomb (M–C) model which involves five input parameters, i.e. two elastic parameters (elastic stiffness E_s and Poisson's ratio ν) and three strength parameters (angle of internal friction φ , cohesion c for soil plasticity and ψ as the angle of dilatancy). As mentioned earlier, the study attempts to address the foundations on hill-slopes of North-Eastern region, which are generally composed of highly weathered rock or soil-rock mixture. It is understood that M–C model falls short in representing such material, which can be better represented by the Generalized Hoek–Brown or Modified M–C models. Owing to the limitation of the FE software in considerations of such constitutive behaviours, an equivalent M–C criteria with equivalent model parameters for the weathered rock mass can be suitably used for the present study, while all the other steps of the numerical model remains exactly the same.

Stages of Analyses

Based on the developed 3D simulation models, several numerical analyses have been conducted in order to investigate the following:

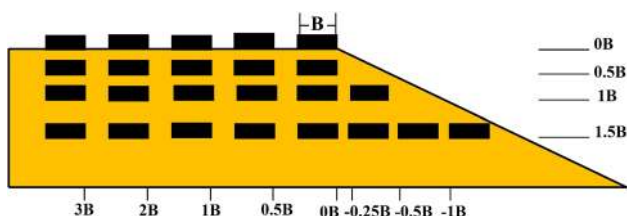


Fig. 5 Locations of surface and embedded footing in a sloping ground

- Validation of the numerical model.
- Convergence study to determine the optimum mesh configuration.
- Effect of the variation of geotechnical and geometrical parameters, namely angle of internal friction of soil (φ), stiffness of soil (E_s), dry unit weight of foundation soil (γ), slope angle (β), footing width (B), setback distance (b) and embedment depth of footing (D).

Results and Discussions

Validation Study

Castelli and Lentini (2012) experimentally investigated the effect of the bearing capacity of shallow foundations on slopes. The investigation had been performed with square footings of width 6, 8 and 10, resting on the sandy slope inside a model tank of dimension 100 cm long, 45 cm wide and 40 cm high. Three setback distances have been used during the experiment ($b = 0.04$ m, 0.12 m, 0.21 m). Load was applied incrementally by a hydraulic jack and was maintained manually with a hand pump. The vertical displacements were measured by means of displacement transducers. Settlement data were recorded using a data acquisition system having a precision of 0.025 mm. All the tests were performed on specimens of Playa Catania (Italy) sand. A series of standard drained shear tests were carried out to evaluate the internal friction angle of the model sand using specimens prepared by dry tamping. The estimated internal friction angle at the relative density of 87% was approximately $\varphi = 38^\circ$, the maximum dry density (γ_{dmax}) was obtained to be 17.50 kN/m³. The test soil bed was constructed in layers, forming a slope angle of 30° at the face.

A 3D FE numerical model is developed to represent the experimental work reported by Castelli and Lentini (2012). In order to identify the optimal meshing configuration for the numerical model, a convergence study had been carried out (considering different footing locations and sizes) with five different meshing schemes (differentiated and represented by their non-dimensional average element length). The non-dimensional average element length is defined as the ratio of the average element length to the largest geometrical dimension of the model. Figure 6 represents the result of the convergence study for a typical footing location ($b = 0.04$ m), and exhibits that beyond a medium mesh, the obtained results are nearly identical; similar result has been obtained for other configurations. Hence, the medium mesh (non-dimensional average element length approximately 0.086) is considered to be optimum for the validation study.

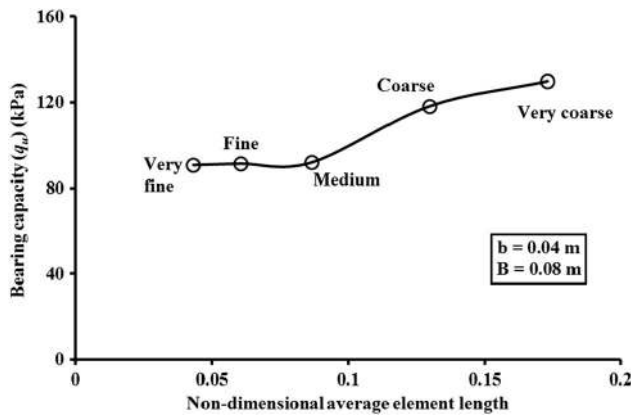


Fig. 6 Convergence study for determining the optimum mesh size

In order to validate the numerical model considering the optimal mesh size, various geometrical configurations related to the footing location and setback distances have been considered for the study. The model dimensions and the material properties have been adopted identical to that of the experimental model considered by Castelli and Lentini (2012). As the stiffness parameters for the experimental model was not specified, the modulus of elasticity ($E_s = 15$ MPa) and Poisson’s ratio ($\nu = 0.3$) has been taken in accordance to the standard references (Keskin and Laman 2013; Naderi and Hataf 2014). Figure 7 represents the comparison of the load-settlement behaviour for a typical geometrical configuration ($B = 0.08$ m, $b = 0.12$ m). A good agreement between the experimental and numerical results can be observed, thus indicating the developed numerical model is suitable for representing the response of such foundations.

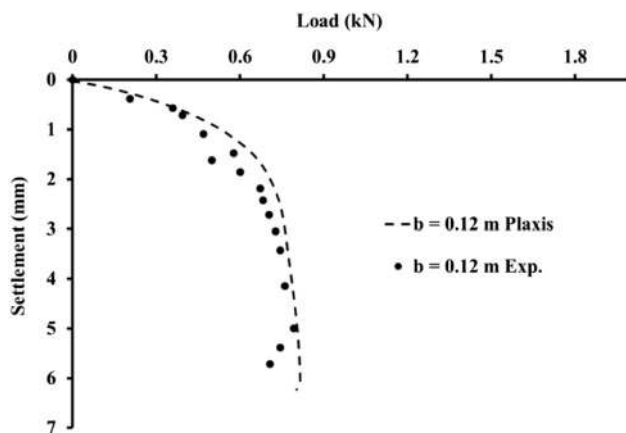


Fig. 7 Validation of the numerical model with experimental investigation by Castelli and Lentini (2012)

Parametric Studies

For footing resting on a sloping ground, the setback distance is perceived as one of the most important governing parameter in the assessment of bearing and deformation characteristics of the footing. The lesser the setback distance, higher is the possibility of failure of the footing exhibiting conditions of distress due to the deformation of the slope face. Hence, in order to highlight the effect of various parameters, a detailed parametric study has been conducted keeping the setback distance as one of the contributing parameters of the simulation., For a footing resting on a sloping ground, five different setback ratios were considered in the analysis, namely $b/B = 0, 0.5, 1, 2$ and 3, and the same is represented in Fig. 5.

As earlier, the numerical simulation of footings resting on sloping ground, with various setback ratios (b/B) and embedment ratios (D/B) had been checked for mesh convergence, the results of which are illustrated in Fig. 8. It can be observed that beyond a medium mesh (average non-dimensional mesh size of nearly 0.14), the obtained results are nearly identical, and hence, all the further studies for the sloping ground have been carried out with the same. To determine the non-dimensional mesh size, the largest dimension of the model for this study has been considered to be the width of the model, i.e. 12 m, which remains invariant for all the simulation scenarios.

Variation of Angle of Internal Friction (ϕ)

Figure 9 illustrates the effect of variation of angle of internal friction (ϕ) on the bearing capacity (q_u). It can be observed that the combined variation of setback ratio and angle of internal friction have significant effect on the

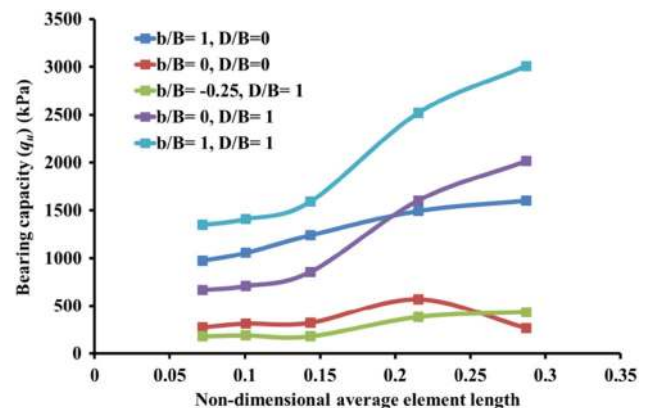


Fig. 8 Convergence study for footing resting on sloping ground for varying b/B and D/B

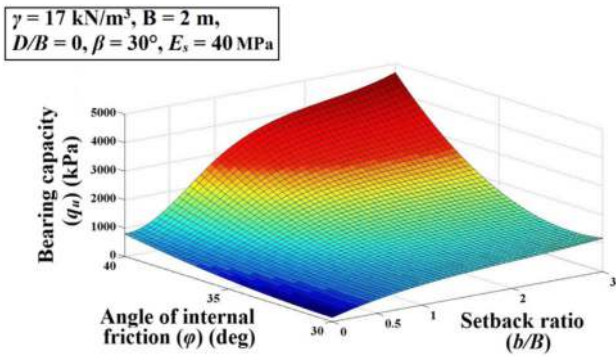


Fig. 9 Variation of q_u with angle of internal friction (ϕ) and setback ratio (b/B)

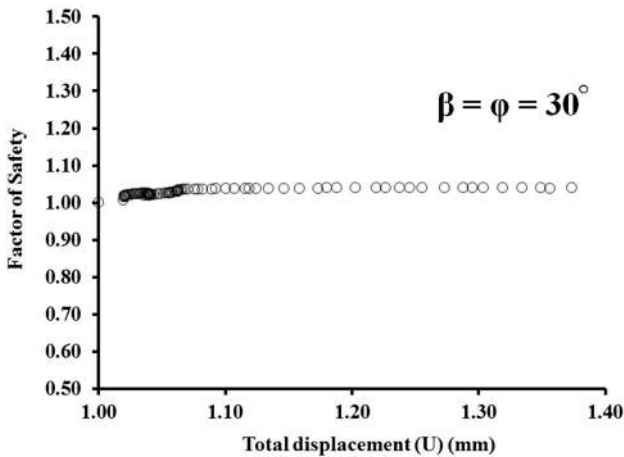


Fig. 10 Safety analysis of a typical slope, $\beta = \phi = 30^\circ$

above estimates. It can be noticed that for any setback ratio, the increase in ϕ resulted in the increase in the magnitudes q_u , the effect being more prominent at higher values of ϕ .

A special case of the variation of angle of internal friction is presented for the case when the magnitude becomes equal to the slope angle. Such a slope remains to be just-stable at the verge of failure, and exhibits a factor of safety (FoS) equal to 1 (one) in its natural state, as shown in Fig. 10. Figure 11 shows the total displacement pattern of such slope in its natural state, exhibiting minimal deformation of the slope face. Such a slope when subjected to minimal loading exhibits an overall failure of the slope, as exhibited in Fig. 12.

Variation of Angle of Slope (β)

Change in the slope angle (β) can significantly alter the stability conditions and bearing capacity characteristics of the footing resting on the sloping ground. A footing exhibits a higher bearing capacity while resting on or near a

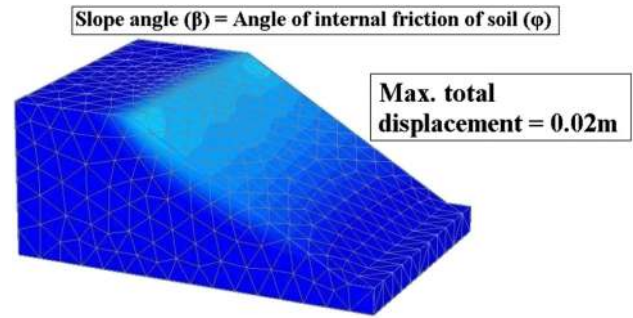


Fig. 11 Total displacement pattern for a slope at its natural state (at incipient failure)

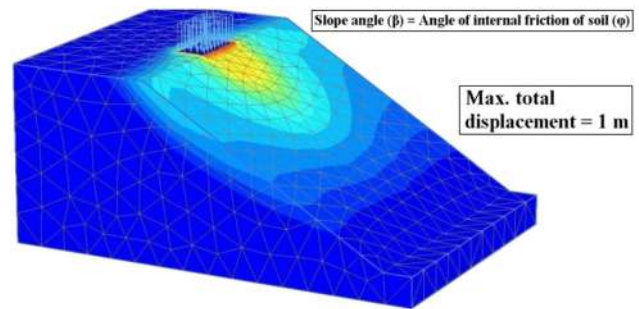


Fig. 12 Overall failure of a slope ($\beta = \phi$) after implementing load on square footing

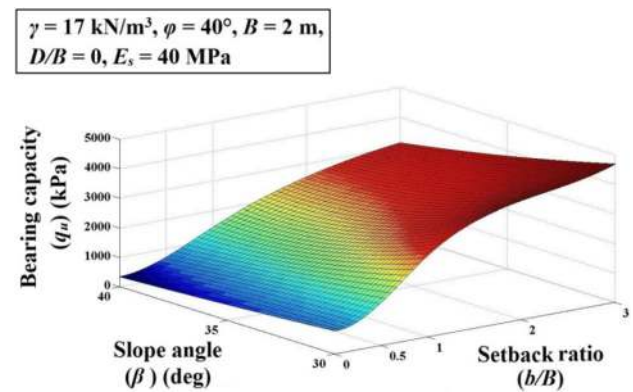


Fig. 13 Variation of q_u with slope angle (β) and setback ratio (b/B)

slope with lesser inclination. Moreover, the natural stability of the slope is governed by the slope angle in relation to the angle of internal friction of the constituent material. For the present study, three different slope angles have been considered namely $\beta = 30^\circ, 35^\circ$ and 40° . It can be observed from Fig. 13 that q_u decreases with the increase in the angle of inclination of the slope. This is attributed to the fact that more steeper is the slope, the zone of passive resistance will be smaller and, hence, less resistance towards failure will be offered by the soil located towards the slope face.

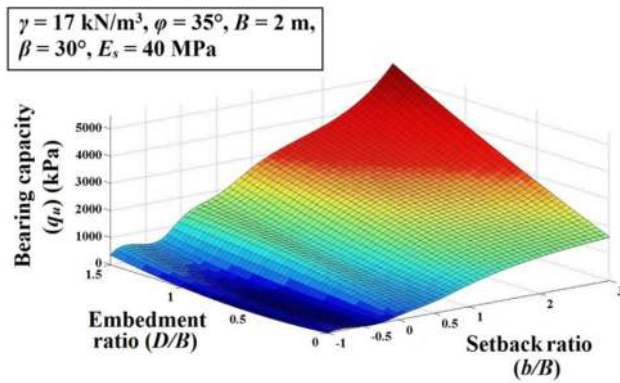


Fig. 14 Variation of q_u with embedment ratio (D/B) and setback ratio (b/B)

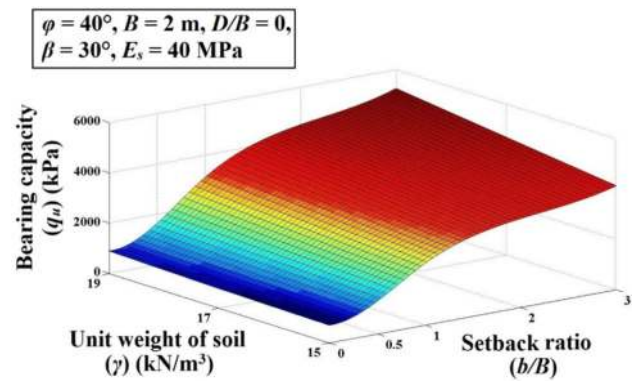


Fig. 16 Variation of q_u with unit weight of soil (γ) and setback ratio (b/B)

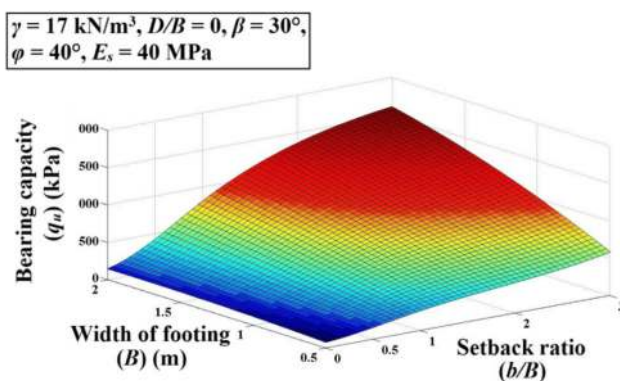


Fig. 15 Variation of q_u with footing width (B) and setback ratio (b/B)

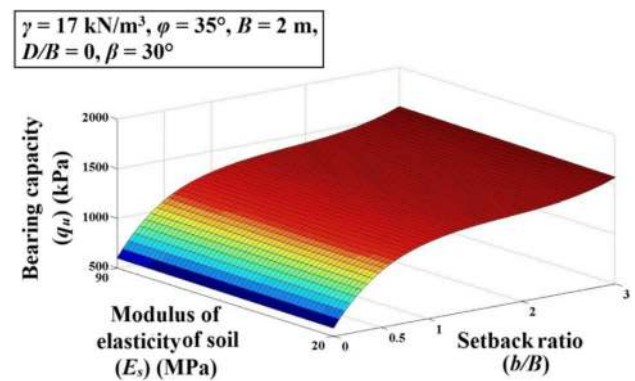


Fig. 17 Variation of q_u with elastic modulus of soil (E_s) and setback ratio (b/B)

Three different embedment ratios were chosen for footing resting on the crest of a sloping ground having D/B were considered to be 0.5, 1 and 1.5, so that the footings can be considered to behave as shallow footings. Figure 14 shows that for any setback distance, the bearing capacity (q_u) increases with the increase in the embedment ratio of footing (D/B), the effect being more prominent when the footing is located away from the face of the slope i.e. the footing exhibits a higher setback distance. The negative setback distances are for the footings located on the face of the slope as exhibited in Fig. 5. Such locations exhibit comparatively low bearing capacity due to the immensely curtailed development of the passive resistance zone towards the slope face.

Variation of Footing Width (B)

Four different footing widths have been chosen namely $B = 0.5, 1, 1.5$ and 2 m. Figure 15 shows the variation of ultimate bearing capacity (q_u) for various footing widths. Increase of ultimate bearing capacity reconfirms the fact

that a greater footing width involves a larger soil domain to support the incumbent load.

Variation of Unit Weight of Soil (γ)

Three different unit weight of the soil has been chosen namely $\gamma = 15, 17$ and 19 kN/m³. Variation of unit weight of soil did not produce significant effect on the bearing capacity (q_u), as exhibited in Fig. 16.

Variation of Elastic Modulus of Soil (E_s)

It is perceived from Fig. 17 that the elastic modulus of soil (E_s) has insignificant effect on bearing capacity (q_u) of soil. It can be seen that the bearing capacity increases with the increase in the setback ratio (b/B), which is rather obvious. From Figs. 9, 13, 14, 15 and 16, it is clear that for a footing located with a lesser setback distance, i.e. located near to the face of the slope, any application of load results in the incomplete development of the resisting passive zone beneath the footing due to the presence of the sloping boundary which fails to provide enough passive

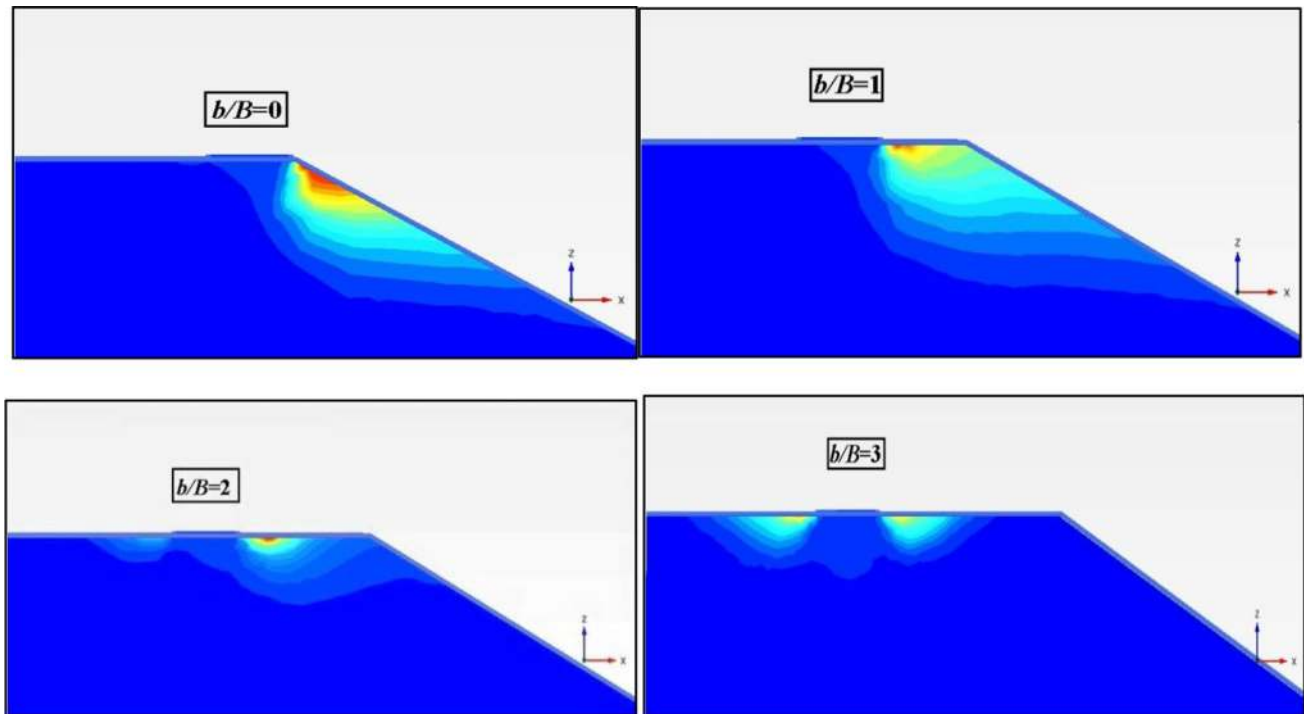


Fig. 18 Formation of passive zones beneath the footing for various setback ratios (b/B)

confinement. With the increase in the setback distance, the formation of the passive zones attains completeness and thus provides more restriction to the lateral movement of the foundation and largely inhibits the loss of confinement. Hence, an increase in the setback distance clearly manifests the increment in the bearing capacity of the footing.

Failure Mechanism of Foundations on Slopes

For footings placed at various setback distances from the slope face, Fig. 18 depicts the role of the sloping face in intersecting the resisting passive zone beneath the footing, and thus reducing the bearing capacity. It is observed that for a footing placed at the crest of the slope ($b/B = 0$), the formation of passive zone is largely one-directional and curtailed by the slope face, due to the dominant free deformation of the soil upon loading of the footing to failure. This phenomenon results in a substantial reduction of the confinement pressure, and hence, diminution of the bearing capacity. As the setback ratio increases, the influencing effect of the slope face on the development of the passive mechanism gradually diminishes, as can be observed from the figure. It is noted that beyond a critical setback ratio $(b/B)_{\text{critical}}$ of 3, the footing behaves as if resting on horizontal ground, wherein the developed stress contours for the passive zone remains unaffected from the influence of the slope face.

Conclusions

Based on the present study, the following significant conclusions are drawn:

- Mesh convergence study aided to define a non-dimensional optimal mesh size for the PLAXIS 3D models so as to obtain accurate solutions from the numerical simulation.
- Bearing capacity increases with the increase in the angle of internal friction for footing resting on sloping ground.
- Bearing capacity increases with an increase of embedment depth of the footing owing to increase in the degree of confinement restricting the movement of the soil towards the sloping face.
- Bearing capacity gets significantly increased with the increase in the footing width.
- Bearing capacity reduces with the increase of slope angle, which is associated with the increased soil movement towards the slope.
- Bearing capacity increases with the increasing setback distance. Beyond a critical setback ratio $b/B = 3$, the footing behaves similar to that on horizontal ground.
- The variation of unit weight and modulus of elasticity of soil has marginal effect on the bearing capacity.

References

Azzam WR, El-Wakil AZ (2015) Experimental and numerical studies of circular footing resting on confined granular subgrade adjacent to slope. *Int J Geomech ASCE* 16(1):1–15

Azzam WR, Farouk A (2010) Experimental and numerical studies of sand slopes loaded with skirted strip footing. *Electron J Geotech Eng* 15:795–812

Bauer GE, Shields DH, Scott JD, Gruspier JE (1981) Bearing capacity of footing in granular slope. In: *Proceedings of the 11th International Conference on Soil Mechanics and Foundation Engineering*, Balkema, Rotterdam, The Netherlands vol 2, pp 33–36

Castelli F, Lentini V (2012) Evaluation of the bearing capacity of footings on slopes. *Int J Phys Model Geotech* 12(3):112–118

Cerato AB, Lutenegeger AJ (2006) Bearing capacity of square and circular footings on a finite layer of granular soil underlain by a rigid base. *J Geotech Geoenviron Eng ASCE* 132(11):1496–1501

Cerato AB, Lutenegeger AJ (2007) Scale effects of shallow foundation bearing capacity on granular material. *J Geotech Geoenviron Eng ASCE* 133(10):1192–1202

Chakraborty D, Kumar J (2014) Seismic bearing capacity of shallow embedded foundations on a sloping ground surface. *Int J Geomech* 15(1):1–8

Choudhury D, Rao KS (2005) Seismic bearing capacity of shallow strip footings. *Geotech Geol Eng* 23(4):403–418

Choudhury D, Rao KS (2006) Seismic bearing capacity of shallow strip footings embedded in slope. *Int J Geomech* 6(3):176–184

El-Sawwaf M (2005) Strip footing behavior on pile and sheet pile-stabilized sand slope. *J Geotech Geoenviron Eng ASCE* 131(6):705–715

El-Sawwaf M (2010) Experimental and numerical study of strip footing supported on stabilized sand slope. *Geotech Geol Eng* 28:311–323

Ghosh P, Choudhury D (2011) Seismic bearing capacity factors for shallow strip footings by pseudo-dynamic approach. *Disaster Adv* 4(3):34–42

Hansen BJ (1970) A revised and extended formula for bearing capacity. *Danish Geotechnical Institute, Bulletin No. 28*, Copenhagen

Keskin MS, Laman M (2013) Model studies of bearing capacity of strip footing on sand slope. *KSCE J Civ Eng* 17(4):699–711

Kumar J, Chakraborty D (2013) Seismic bearing capacity of foundations on cohesionless slopes. *J Geotech Geoenviron Eng ASCE* 139(11):1986–1993

Kumar J, Ghosh P (2006) Seismic bearing capacity for embedded footing on sloping ground. *Geotechnique* 56(2):133–140

Kumar SVA, Ilamparuthi K (2009) Response of footing on sand slopes. *Indian Geotechn Conf* 77:622–626

Kumar J, Rao VBKM (2003) Seismic bearing capacity of foundations on slopes. *Geotechnique* 53(3):347–361

Lavasan AA, Ghazavi M (2014) Failure mechanism and soil deformation pattern of soil beneath interfering square footings. *Numer Method Civ Eng* 1(2):48–56

Meyerhof GG (1957) The ultimate bearing capacity of foundation on slopes. In: *Proceedings of the 4th International Conference on Soil Mechanics and Foundation Engineering I*, pp 384–386

Naderi E, Hataf N (2014) Model testing and numerical investigation of interference effect of closely spaced ring and circular footings on reinforced sand. *Geotext Geomembr* 42:191–200

NDMA (2013) Catalogue of building typologies in India: seismic vulnerability assessment of building types in India. A report submitted by the Seismic Vulnerability Project Group of IIT Bombay, IIT Guwahati, IIT Kharagpur, IIT Madras and IIT Roorkee to the National Disaster Management Authority

Pain A, Choudhury D, Bhattacharyya SK (2016) The seismic bearing capacity factor for surface strip footings. *Geotechn Spec Publ ASCE* 269:197–206

Shields DH, Scott JD, Bauer GE, Deschenes JH, Barsvary AK (1977) Bearing capacity of foundation near slopes. In: *Proceeding of the 10th International Conference on Soil Mechanics and Foundation Engineering*, Tokyo, Japan, vol 2, pp 715–720

Shukla RP, Jakka RS (2016) Discussion on experimental and numerical studies of circular footing resting on confined granular subgrade adjacent to slope by WR Azzam and AZ El-Wakil. *Int J Geomech* 17(2):1–3

Terzaghi K (1943) *Theoretical soil mechanics*. Wiley, New York

Turker E, Sadoglu E, Cure E, Uzuner BA (2014) Bearing capacity of eccentrically loaded strip footings close to geotextile-reinforced sand slope. *Can Geotech J* 51:884–895

Vesic AS (1973) Analysis of ultimate loads of shallow foundation. *J Soil Mech Found Div ASCE* 99(SM1):45–73

Yu L, Liu J, Kong XJ, Hu Y (2010) Three-dimensional large deformation FE analysis of square footings in two-layered clays. *J Geotech Geoenviron Eng ASCE* 137(1):52–58

Zhu M, Michalowski RL (2005) Shape factors for limit loads on square and rectangular footings. *J Geotech Geoenviron Eng ASCE* 131(2):223–231